A Compact and Robust Variable Reluctance Actuator for Grasping Applications

Norbert C. Cheung
Department of Electrical Engineering,
Hong Kong Polytechnic University,
Hunghom, Kowloon, Hong Kong
Eencheun@polyu.edu.hk

Abstract - **Variable reluctance actuators have a simple and robust structure, and they are widely used as a low cost switching actuators in many applications. However, they have not gained widespread acceptance as proportional actuators due to their inherent nonlinear control characteristics. In this paper, a robust, compact and easy-to-manufacture grasping actuator based on variable reluctance (VR) technology is presented. Using a novel control strategy, the actuator can be operated in position, velocity, and force control modes. This makes the actuator ideal for high speed grasping of delicate objects in robotics applications. The paper describes the construction, and operating principle of the VR grasping finger. It also describes the fabrication and the measurement of essential electrical and mechanical characteristics of the actuator. Then, a novel nonlinear control algorithm for multi-mode control of position, velocity, and force has been proposed. The proposed algorithm is implemented on a DSP system to control the VR grasping finger in various motion control modes. Results from the implementation show that the VR grasping finger can be controlled with a high degree of speed and accuracy, and the application of force on the object in force control mode is stable and accurate.**

I INTRODUCTION

Variable reluctance (VR) actuator has a robust and simple structure and its manufacture cost is much lower than similar permanent magnet moving coil device. However, this kind of proportional actuator has not gained widespread acceptance, due to its nonlinear magnetic and electrical characteristics. A VR proportional actuator is much more difficult to control than a moving coil actuator. During the past few years there has been a renewed interest in VR actuators [1], party due to the advancement of high speed power switches, computing devices, and advanced control algorithms. In spite of these advancements, most publications are predominantly concerned with velocity control of multi-phase rotary switched reluctance motors [2,3].

The author has previously conducted some work on the modelling, control, and position estimation of VR solenoid actuators [4,5,6]. This paper is an extension of the previous work into the area of grasping control for VR actuators. In this paper, a novel "grasping finger" actuator based on VR principle is developed. The VR grasping finger has the same simple and robust structure as other VR actuators, and it can be used for high speed pick and place of delicate objects.

The VR grasping finger has been designed, fabricated and tested, and its essential electromechanical characteristics have been measured. To provide effective motion and force control for the actuator, a novel nonlinear control strategy has been developed.

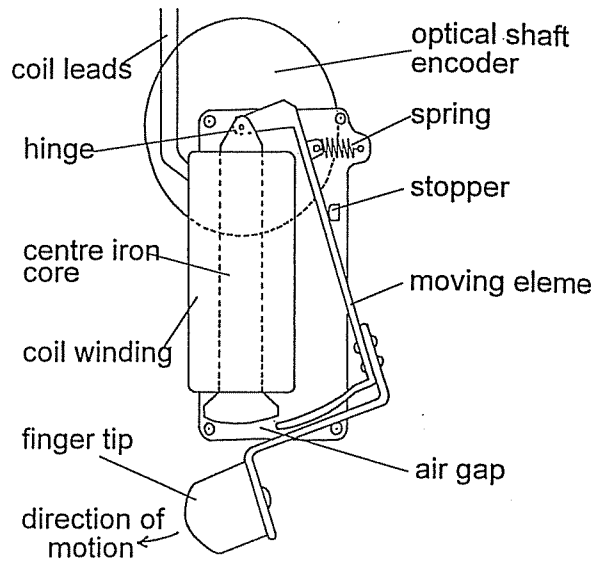

Fig.1 The variable reluctance finger

The developed control algorithm is then implemented on a DSP control system, to control the VR actuator in position, velocity and force control modes.

Preliminary results show that the VR grasping finger has a high response speed with high accuracy in both position and force control modes. Results indicate that the VR grasping finger provides a performance level which is similar to voice coil grippers, while at the same time gives additional advantages of low cost, simple construction, and robust construction.

Presently, only one VR grasping finger has been fabricated and studied. However, there is no limitation on the number of fingers used in coordination with each other. Due to the small and convenient size of the grasping finger, combination two or more VR fingers in robotics grasping applications can be achieved without much difficulty.

Section II describes the design and the electrical-mechanical behavior of the actuator; section III proposes a nonlinear position and force control algorithm for multi-mode control of the grasping finger. Finally, section IV describes the implementation and result of the VR actuator.

II CONSTRUCTION OF THE VR GRASPING FINGER

Fig. 1 shows the construction diagram of the VR grasping finger. It consists of a coil with a laminated magnetic core at centre. The moving element hinges on the upper end of the laminated core, and is spring loaded to allow the fingertip to move outwards when unenergised. The spring also ensures good magnetic circuit contact between the moving part and the stationary element. A

0-7803-4503-7/98/$10.00 1998 IEEE

miniature rotary optical encoder is mounted on the hinge of the VR grasping finger to sense the angular displacement of the moving element. The moving element is machined from annealed "Carpenter 430FR" metal sheet. The maximum angle of rotation for the moving element from its unaligned position to its fully aligned position is 22.5°. The overall length of the VR grasping finger is below 8cm, and the maximum travel of its fingertip is 2.5cm.

Unlike d.c. voice coil actuator, the VR actuator's characteristics are highly dependent on the nonlinear behavior of its magnetic circuit. Before effective control of the VR grasping finger can be achieved, a study on the actuator's magnetic flux behavior is required.

The voltage equation of the VR grasping finger can be written as:

$$V = Ri + \frac{d\lambda}{dt} \tag{1}$$

where V is the voltage applied to the coil. R, i, and λ are coil resistance, current of coil, and flux linkage respectively.

Since λ is dependent on current of the coil and the angle of alignment θ, (1) can be expanded as:

$$V = Ri + \frac{\partial\lambda(\theta,i)}{\partial i}\cdot\frac{di}{dt} + \frac{\partial\lambda(\theta,i)}{\partial\theta}\cdot\frac{d\theta}{dt} \tag{2}$$

On the mechanical side, the VR grasping finger can be represented by a second order system:

$$I\ddot{\theta} = T - K_s\theta \tag{3}$$

K_s is the torque constant produced by the spring on a particular attachment location, whereas T and I are the torque and inertia of the actuator.

The torque produced by the moving element can be calculated from the coenergy W' of the actuator, as (4)-(5) below:

$$T = \frac{\partial W'(\theta,i)}{\partial\theta} \tag{4}$$

$$W'(\theta,i) = \int_0^i \lambda(\theta,i)di \tag{5}$$

From (4) and (5) the instantaneous torque can be rewritten as:

$$T = \frac{\partial\lambda(\theta,i)}{\partial\theta}\cdot i \tag{6}$$

From (1)-(6), a set of state equations can be formed:

$$\frac{dx}{dt} = v \tag{7}$$

$$\frac{dv}{dt} = T(\theta,i) - K_s\theta \tag{8}$$

$$\frac{di}{dt} = \left(V - Ri - E(\theta,i)\cdot\frac{d\theta}{dt}\right)\cdot L(\theta,i)^{-1} \tag{9}$$

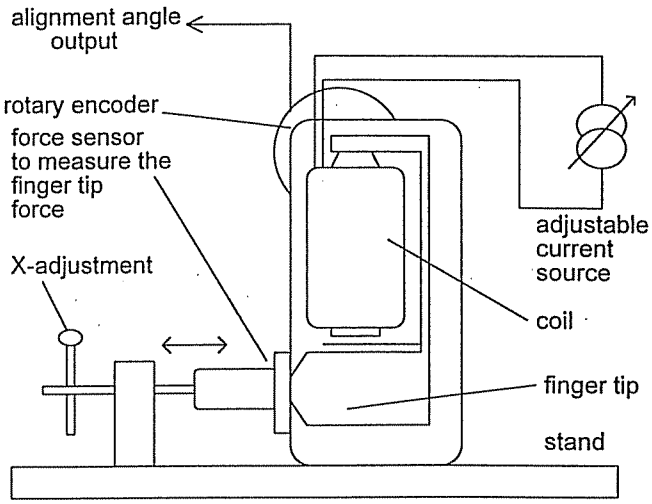

Fig.2 Setup for the measurement of static force

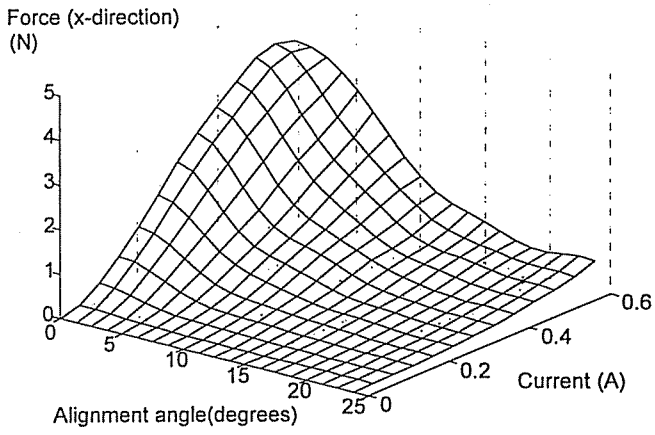

Fig.3 The static force profile of the VR grasping finger

where $E(\theta,i)$ and $L(\theta,i)$ are the back e.m.f. constant and the incremental inductance of the actuator, and they can be expressed as:

$$E(\theta,i) = \frac{\partial(\theta,i)}{\partial\theta} \tag{10}$$

$$L(\theta,i) = \frac{\partial(\theta,i)}{\partial i} \tag{11}$$

Presently, no force sensor is installed on the fingertip of the VR actuator, and force control is executed in open loop mode. Since stationary grasping force does not involve any dynamics, therefore the force generated on the fingertip is determined by the alignment angle θ and the current of the coil i as described in (6). To determine the actual grasping force along the x direction, a measurement setup, shown in Fig. 2, is used to measure the static force of the VR finger at different horizontal positions and currents. The measurements include spring effect and gravity. Fig. 3 shows the measurement result.

The result in Fig.3 is used as a look up table in the force control mode, and is expressed by (12):

$$FingerTipForce(x\text{-}direction) = F_x(\theta,i) \tag{12}$$

The VR grasping finger has a maximum moving angle of 22.5° (or ±11.25°); the transformation from angular torque to linear force will produce a maximum nonlinearly error of 4%, therefore it is feasible to use the same force look up table for (8) and (12). Their relation is shown in (13).

$$T(\theta,i) \cong F_x(\theta,i) \cdot K_{lns} \tag{13}$$

where $F_x(\theta,i)$ is the graph shown in Fig. 3, and K_{lns} is a constant for rotary-linear transformation.

Unlike rotary VR motors which spins at very high speed, the VR finger has a limited travel and its controlled motion is comparatively slow. Therefore, the back e.m.f. constant $E(\theta,i)$ in (9) can be approximated to zero. Also, the force look up table $F_x(\theta,i)$ of (12) has already included spring effect and gravity. The state equations of (7)-(9) can be simplified to (14)-(16).

$$\frac{dx}{dt} = v \tag{14}$$

$$\frac{dv}{dt} = K_x(\theta,i) \cdot K_{transform} \tag{15}$$

$$\frac{di}{dt} = \frac{V - Ri}{L(\theta,i)^{-1}} \tag{16}$$

The incremental inductance $L(x,i)$ of the VR actuator at various angles and currents are obtained from the phase differences between currents and voltages measurements of the actuator. The measurement setup is similar to the measurement of the static force described in the previous page. The only differences are (i) clampers are used to station the moving element during the measurements, and (ii) a d.c. biased a.c. voltage is fed to the coil, to provide an a.c. signal with d.c. current offset. Fig.4 shows the set up for the measurement of incremental inductance.

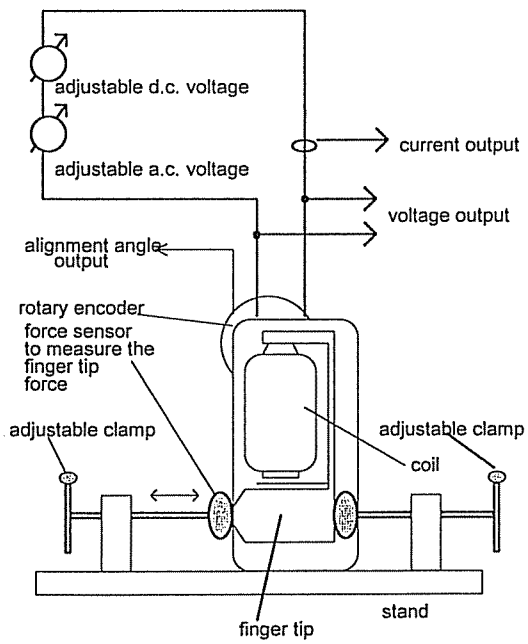

Fig.4 Measurement of incremental inductance

III CONTROL ALGORITHM FOR THE VR FINGER

To enable fast grabbing of the object with minimal impact on the object, the VR grasping finger has three modes of operation.

Firstly, the fingertip moves from its fully opened position to a predefined location using high-speed point to point motion. Then, a relatively low constant speed is executed for object search until the fingertip hits object. Once an impact is detected, a constant force is applied to the VR finger to grasp the object firmly.

The full motion profile is shown in Fig. 5. An S-shaped trajectory profile is used for the high-speed point to point motion. Once the controller has registered that the desired location is reached, the controller will switch to velocity search mode. The velocity search mode is a linear trajectory profile. Once an object hit is registered, the controller will switch to force control mode. An object hit is detected by monitoring the difference between the desired position and the actual position. When an object hit occurs, this difference will increase above a predefined threshold level.

Due to the above situation, the controller is required to operate in (i) trajectory tracking mode, (ii) constant velocity mode, and (iii) constant force mode, and must be able to switch between these modes. On top of this, the force behavior and the inductance characteristics of the VR actuator, shown in (14)-(16) are nonlinear. To overcome the nonlinearities, a controller with a force-to-current lookup table $i(F_x,\theta)$ (i.e. reciprocal function of $F_x(\theta,i)$) is employed to compensate the nonlinear force behavior, and a very fast inner current loop is used to compensate the nonlinear characteristics of incremental inductance. For the latter case, measurements of incremental inductance indicate that the actuator becomes nonlinear only when it is in the saturated region. Even in its saturated region, it is still a continuous function. Therefore a fast PD current controller can adequately compensate the mild nonlinear behavior.

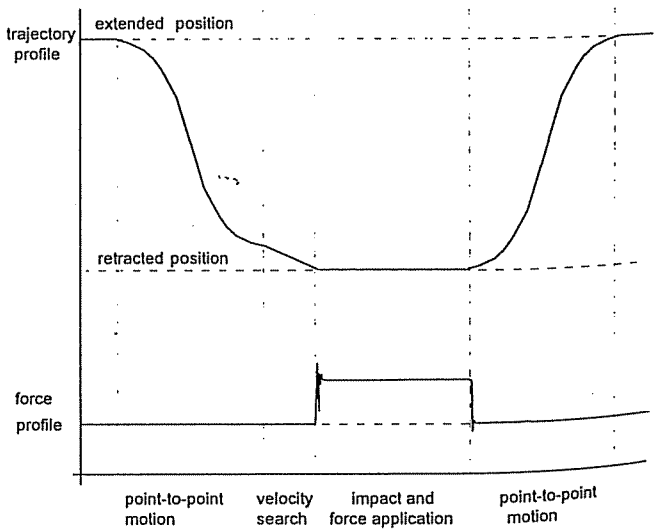

Fig. 5 The full motion profile

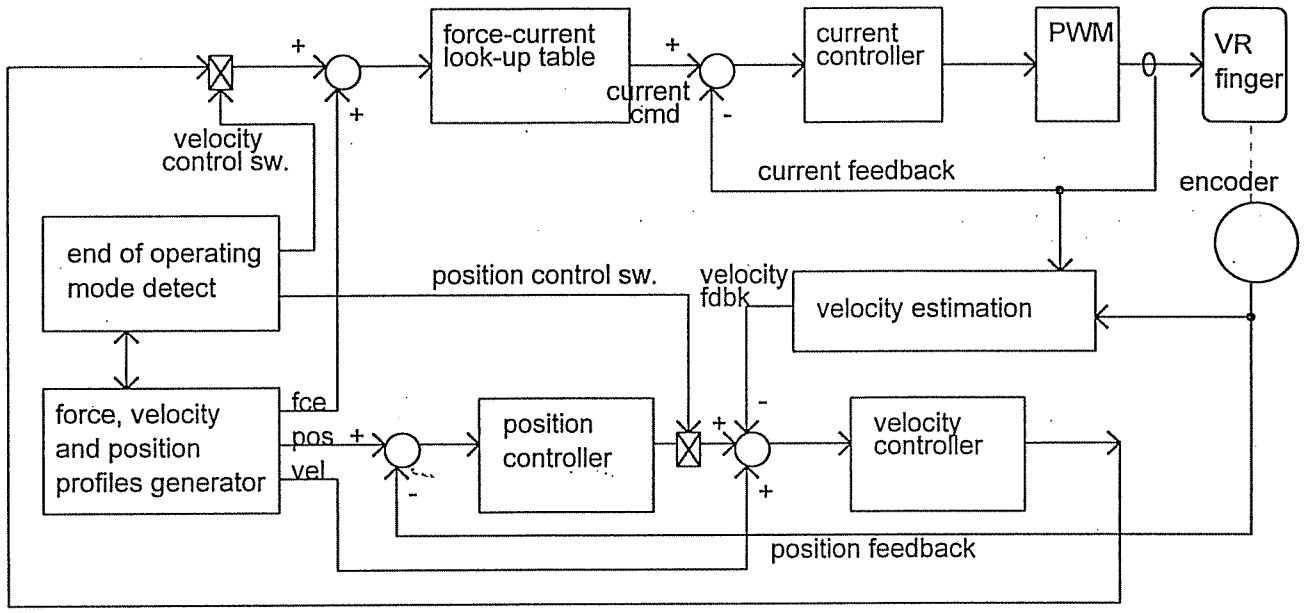

Fig.6 The overall control algorithm

The force to current look up table $i(\theta,F_x)$ is constructed in software as a 20×20 matrix. Two-dimension linear interpolation is used to estimate the intermediate values.

The overall control structure is shown in Fig. 6. The switch from position tracking mode to constant velocity mode is made when end-of-travel is reached. The switch from constant velocity mode to constant force mode is made when there is a large error deviation between the command position and the actual position

IV IMPLEMENTATION AND RESULTS

The overall system has been implemented on a DSP control development system, with a MOSFET bridge driver as the output device and a rotary incremental encoder as the position feedback. The overall setup is shown in Fig.7. A piezo-electric force sensor is used for force detection, and a miniature Hall effect transducer is used for current measurement. The optical encoder has a resolution of 0.18°.

Fig 8. shows the accuracy of the VR finger in trajectory tracking mode. The result shows that the tracking performance of the VR grasping finger is fast and accurate. Fig.9 shows the force profiles of the actuator at various angles. A step function force command is applied to the actuator a t=0. In spite of open loop control, the result shows that the grasping force can be stablised within 0.25s from rest.

Fig.10 shows the full grasping action of the actuator. During this test, the actuator is actuator tapping on a hard vertical surface. The result shows that the actuator can follow the trajectory command closely, as well as providing a constant and accurate grasping force on the target object. Due to the light mass of the actuator's finger and the appropriate search speed, there is less than 15% force overshoot when the actuator's finger hits the object.

V CONCLUSION

This paper has presented a novel VR grasping finger that has a compact, simple and robust construction. A novel but simple control algorithm which takes into the account of the actuator's nonlinear control behavior has been proposed. To ensure fast grasping of delicate objects, the VR grasping actuator operates in three distinct modes (position tracking mode, velocity search mode, and constant force mode). In this investigation, the actuator has been designed and fabricated, and its electrical and force characteristics have been measured. A novel control algorithm for the grasping action of the VR actuator is proposed. The proposed control algorithm is implemented on a DSP control system to drive the actuator. Results show that the VR grasping finger can be control for a full grasping motion with high speed, accuracy, and stability.

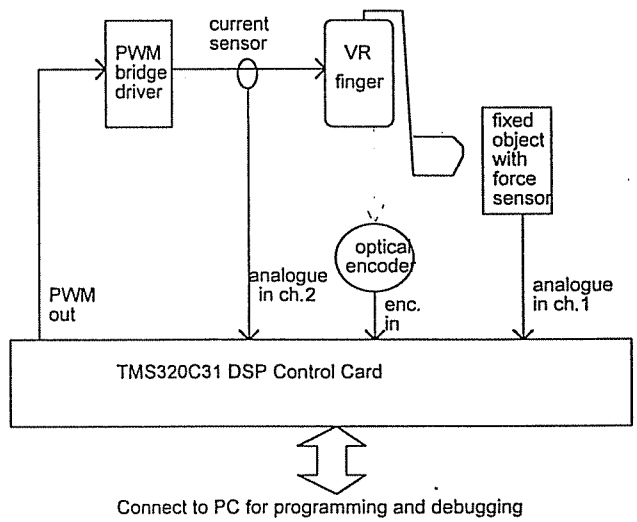

Fig. 7 Setup of the whole system

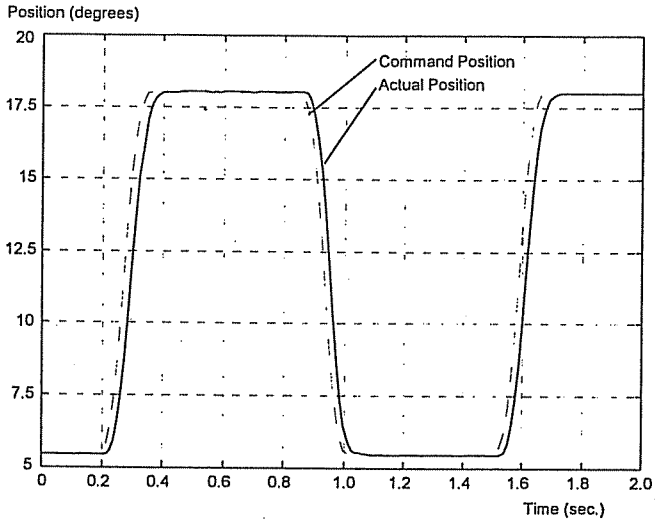

Fig. 8 Actual performance - trajectory tracking mode

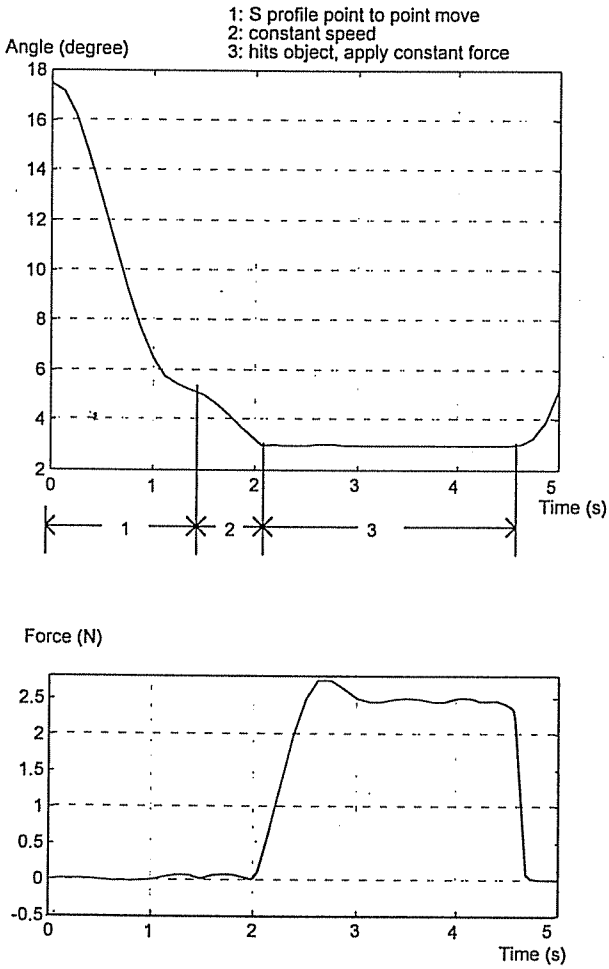

Fig. 10 Actual performance – full grasping action

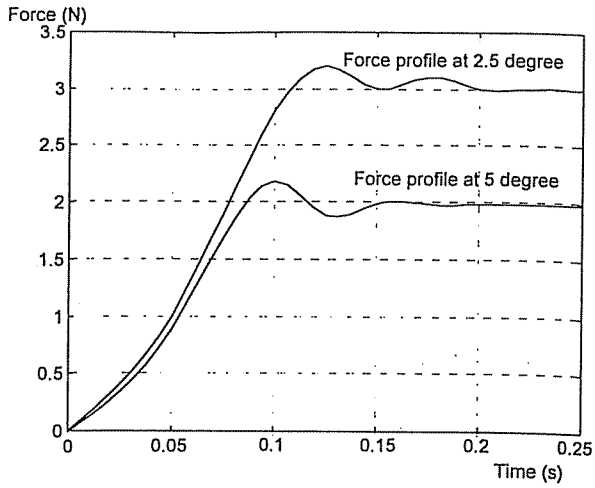

Fig. 9 Actual performance – force profile at a stationary angle

VI REFERENCES

[1] T.J.E. Miller, "Switched reluctance motor and their control", Magne Physics Publishing and Clarendon Press, Oxford, 1993.

[2] D.G. Taylor, "An experimental study on composite control of switched reluctance motors", IEEE Control Systems Magazine, Vol 11, Iss 6, p31-36, Feb 1991.

[3] A.A. Goldenberg, I. Laniado, P. Kuzan, C. Zhou, "Control of switched reluctance motor torque for force control applications", IEEE Trans. on Industrial Electronics, Vol 41, No 4, p461-466, August 1994.

[4] K.W. Lim, N.C. Cheung, and M.F. Rahman, "Proportional control of a solenoid actuator", IEEE Proc. on Industrial Electronics Society Annual General Meeting, IECON'94, Vol 3, p2045-2050, Bologna, Sep 1994.

[5] M.F. Rahman, N.C. Cheung and K.W. Lim, "Conversion of a switching solenoid to a proportional actuator", Transactions of IEE Japan, Vol 116, Pt D, No 5, May 1996, pp531-537.

[6] M.F. Rahman, N.C. Cheung and K.W. Lim, "Position estimation in solenoid actuators", IEEE Transactions on Industry Applications, Vol 32, No.3, May/Jun 1996, pp 552-559.